Metal Dilution Effects on the Thermal and Light-Induced Spin Transition of Iron(II) in the Three-Dimensional Coordination Polymer $[Fe_xZn_{1-x}(pyrazine)(Pt(CN)_4)]$

Mame Seyni Sylla, Chérif Baldé, Nathalie Daro, Guillaume Chastanet

Journal de la Société Ouest-Africaine de Chimie

J. Soc. Ouest-Afr. Chim.(2017), 043 : 37 - 47

22ème Année, Juin 2017

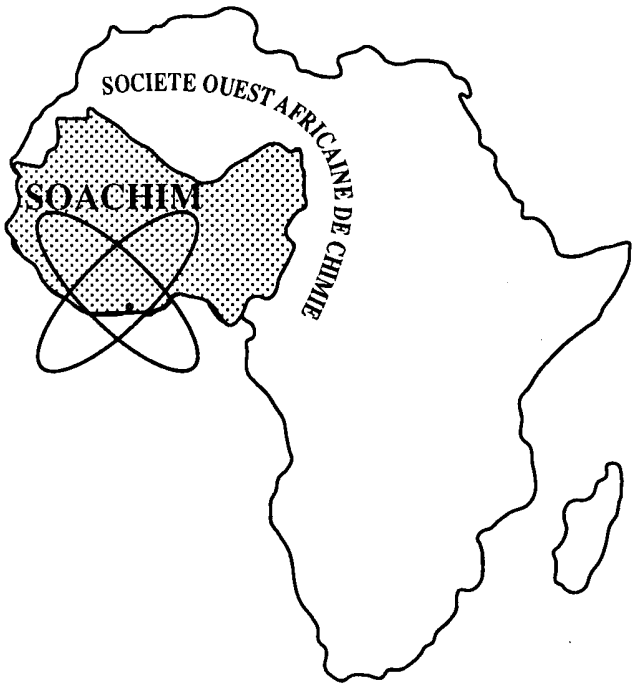

ISSN 0796-6687

Code Chemical Abstracts : JSOCF2

Cote INIST (CNRS France) : <27680>

Site Web: **http://www.soachim.org**

Metal Dilution Effects on the Thermal and Light-Induced Spin Transition of Iron(II) in the Three-Dimensional Coordination Polymer $[Fe_xZn_{1-x}(pyrazine)(Pt(CN)_4)]$

Mame Seyni Sylla[1,2], Chérif Baldé[1*], Nathalie Daro[2], Guillaume Chastanet[2*]

[1] Laboratoire de Chimie et Physique des Matériaux (LCPM) Université Assane Seck de Ziguinchor, BP 523, Sénégal
[2] CNRS, Univ. Bordeaux, ICMCB UPR9048, 87 Avenue du Dr. Schweitzer, F-33600 Pessac, France;

(Reçu le 22/05/2017 – Accepté après corrections le 10/09/ 2017)

Abstract: The effects of metal dilution on the spin-crossover behavior on the three-dimensional coordination polymer [Fe(pyrazine)(Pt(CN)4)] have been studied in the mixed-crystal series $[Fe_xZn_{1-x}(pyrazine)(Pt(CN)_4)]$ ($0 \leq x \leq 1$), using magnetic and photomagnetic measurements. For all the materials investigated, the thermal spin-crossover properties, $T_{1/2}$, were measured and the stability of the photoinduced high-spin states was probed through determination of the T(LIESST) values associated with the light-induced excited spin-state trapping (LIESST) effect. Whereas the neat polymeric $[Fe^{II}(pz)(Pt(CN)_4)]$ (pz = pyrazine) compound shows an abrupt spin transition centered at room temperature, it has been found that $T_{1/2}$ decreases with the metal dilution. Similarly, dilution tends to decrease the hysteresis width and smoothen the transition curves: when x changes from 1 to 0.27, the transition temperature varies from 282 to 237 K in the cooling mode and from 308 to 237 K in the heating mode. The hysteresis, which is 26 K for $x = 1.00$, vanishes for $x = 0.27$. All the mixed-compounds exhibit LIESST effect. These results were discussed taking into account the relative sizes of Zn(II), high-spin Fe(II), and low-spin Fe(II) ions and compared with previous results.

Keywords: *Spin Crossover (SCO); Dilution effects; Metal-coordination chemistry; LIESST; Iron(II)*

Effets de la dilution sur les propriétés de transition de spin thermiques et photo-induites du Fer (II) dans le polymère de coordination tridimensionnel $[Fe_xZn_{1-x}(pyrazine)(Pt(CN)_4)]$

Résumé: Les effets de la dilution sur les propriétés de transition de spin du polymère de coordination tridimensionnel [Fe(pyrazine)(Pt(CN)4)] ont été étudiés dans la série de composés mixtes $[Fe_xZn_{1-x}(pyrazine)(Pt(CN)_4)]$ ($0 \leq x \leq 1$), en utilisant des mesures magnétique et photomagnétique. Pour tous les matériaux étudiés, les propriétés de transition de spin thermique, $T_{1/2}$, ont été étudiées et la durée de vie de l'état photo-induit haut spin a été évaluée par détermination des valeurs T(LIESST) associées à l'effet LIESST. Alors que le composé polymérique pur [Fe(pz)(Pt(CN)4)] (pz = pyrazine) révèle une transition de spin abrupte centrée autour de la température ambiante, il a été observé une diminution progressive de $T_{1/2}$ avec une dilution croissante : lorsque le taux de dopage, x, passe de 1 à 0,27, la température de transition varie de 282 à 237 K en mode refroidissement et de 308 à 237 K en mode chauffage. L'hystérésis, large de 26 K pour x = 1,00, disparaît pour x = 0,27. Ces résultats ont été discutés en tenant compte de la taille relative des ions Zn(II), des ions Fe(II) haut spin et des ions Fe(II) bas spin puis comparés aux résultats rapportés antérieurement.

Mots clés: *Transition de Spin; Effets de la dilution; Chimie de Coordination; LIESST; Fer(II)*

[*] *Correspondence:* cbalde@univ-zig.sn and guillaume.chastanet@icmcb.cnrs.fr

1. Introduction

In principle, Spin-crossover (SCO) systems are a class of inorganic coordination compounds with a central metal ion of d^4 to d^7 electronic configuration. Depending on the ligand field strength in the related complexes, two different electronic configurations can be observed and a transition between these two configurations can be induced by several external stimuli such as temperature, light, pressure… This phenomenon is mainly observed in d^6 iron(II)-based molecular complexes, mostly those with a $Fe^{II}N_6$ coordination environment. For these systems, the SCO occurs between the high-spin (HS) quintet state (t_{2g}^4 e_g^2 ($^5T_{2g}$, S = 2)) and the low-spin (LS) singlet state (t_{2g}^6 e_g^0 ($^1A_{1g}$, S = 0)).[1-6] The ligands for such spin-crossover complexes are chosen to provide a zero-point energy difference between the electronic states of minimum and maximum spin multiplicity on the order of magnitude of thermal energies. Thus the low-spin (LS) state with a maximum number of paired d-electrons and the high-spin (HS) state with maximum spin multiplicity are populated in thermal equilibrium. [7] In fact, the competition between the electron pairing energy, the energy splitting between the t_{2g} and e_g orbitals, the structural reorganization, and the entropy effects are balancing the stability of the LS and HS states at thermal equilibrium [8]. The physical phenomenon obeys to an intramolecular electronic transfer between LS and HS, which may be induced by application of various external stimuli such as temperature, pressure, magnetic field or light irradiation. [2,6,9]

Along the LS → HS conversion, electrons populated antibonding e_g orbitals that disfavor the metal-ligand bond leading to an increase of volume of the coordination sphere. Then, strong structural rearrangements occur due to the difference in volume between the large HS state and the small LS state. [10,11] This volume change, which could be anisotropic, propagates to the solid network through intermolecular interactions that determine the cooperative character of the SCO. Highly cooperative materials are usually characterized by hysteretic behaviors leading to memory effect. Since molecular electronics is based on bistability that refers to the ability of a compound to be observed in two electronic states of a certain range of some external perturbation: binary coding (0-1),[6] the subsequent changes of physical properties such as optical, magnetic, electric… along the SCO phenomenon offer an exciting opportunity to use molecular compound for information storage at nanometer scale operating at room temperature. [2,9,12-16]

The optical switching is particularly regarded since ultrafast switches (femtoseconds) can be achieved. [17] Light can reversibly write and erase the LS and HS states according to the direct or reverse light-induced excited spin state trapping (LIESST) effects. [18-20] The potential use of optical switching in data storage and display devices [6,14,21-23] has raised major interest since the discovery of LIESST effect. [18] Thus, many investigations have been conducted since the discovery of LIESST effect to understand and identify the parameters governing the lifetime of the photo-induced states. The role of intermolecular interactions has been investigated through the influence of the metal dilution in mixed $[Fe_xM_{1-x}]$ complexes with various metals M. [24-41] Diluting the material with non-spin crossover metal sites disrupts the lattice cooperativity, resulting in more gradual spin crossover behavior. Moreover, the size of the dopant ion has a huge effect of the SCO properties. Indeed, ions with ionic radii close to or bigger than the ionic radius of the HS Fe(II) induces a negative internal pressure that favors the state of bigger volume that is HS. We have studied extensively the effect of metal dilution on the LIESST temperature. This T(LIESST) temperature records the limit above which the photo-induced HS state cannot be observed with classical techniques (typically the ones who have timescale detection of the minute). At the end of numerous studies, we evidenced that the thermal spin crossover regime is mainly governed by the thermodynamics and cooperative interactions while the photo-induced HS state lifetime is mainly controlled at the molecular scale by the local environment. [42,43] In other words, while changes in counter-anions, solvent, ligands substituent… strongly affect the T(LIESST) value, metal dilution that reduces the cooperativity does not modify it in a huge way. [32-40] Cooperativity does not influence the HS state stability, in agreement with the Hauser's works and theoretical simulations of T(LIESST). [42,43,44,45,46] Chemical parameters such as rigidity and distortion of the coordination sphere were identified to be of importance in the T(LIESST) increase leading to T(LIESST) shift from 60 K in the late 90's to 130 K for a pure iron(II) SCO materials in the last 10 years [47,48] and even 150 K in Prussian Blue analogues. [49,50] The record is today found for a molecular cluster with a value of about 180 K. [51]

Due to the strong structural reorganizations

along the SCO, the rigidity of the network can prevent the light-induced SCO. Highly cooperative compounds are often associated with poorly efficient LIESST effect. Two strategies are followed to increase the LIESST efficiency. The first one is the solid solutions approaches. By introducing non SCO ions within the structure, defaults are inserted and the cooperativity is lowered. This has allowed to increase the LIESST effect with the drawback of losing hysteretic behavior.[40] A second strategy consists in inserting flexible units as ligands in the structure to induce a competition between ferroelastic (cooperativity) and antiferroelastic (flexibility) interactions leading to an elastic frustration.[52] This has led to some multistep spin crossover hysteresis and efficient photoswitching.[53-55] This is particularly the case of the [Fe(pz)(Pt(CN)$_4$)] (pz = pyrazine) three dimensional compound that exhibit an hysteresis at room temperature but a very weak life-time of the photo-induced state.[56] Introducing flexible ligands favored efficient photoswitching.[54,56]

In the present work, we wanted to investigate the solid solutions approach to this [Fe(pz)(Pt(CN)$_4$)] compound to see if LIESST effect can be enhance in such systems. Up to now, the only solid solutions undertaken on [Fe(pz)(Pt(CN)$_4$)] were performed with only Ni(II) and Co(II) without looking at the LIESST effect. [30,31] The main objective of the present work is therefore to study experimentally metal dilution effects on the properties of spin-crossover polymers. To accomplish this goal, we decided to investigate for the first time, Zn(II) metal dilution effects on the three-dimensional coordination polymer [Fe(pz)(Pt(CN)$_4$)] using magnetic susceptibility and photomagnetic measurements, powder X-ray diffraction (PXRD) and Differential Thermal Analysis.

This complex belongs to a family of compounds of the formula [Fe(pz)(Pt(CN)$_4$)].nH$_2$O, which are known to exhibit an abrupt thermal spin transition, well defined with a large hysteresis loops (≈ 20-30 K), when desolvated. [30,31] The HS crystal structure of the complex (with n = 2) has been determined by PXRD. [30] This structure is tetragonal (P4/m) and consists of planar polymeric sheets formed from square-planar tetracyano-metalate ions bridged by six-coordinate Fe(II) ions. The iron ions are bridged by bidentate pyrazine ligands leading to a three-dimensional network (**Figure 1**).

2. Experimental section

2.1. Chemicals

The preparation of the pure compound has been described previously by Niel et al. [30] The samples of diluted compounds [Fe$_x$Zn$_{1-x}$(pyrazine)(Pt(CN)$_4$)] were prepared according to the same procedure, replacing the Fe(II) FeCl$_2$. 4H$_2$O by a mixture of Fe(II) FeCl$_2$.4H$_2$O and Zn(II) ZnCl$_2$.6H$_2$O in given ratios (15%, 30%, 51%, 73%, 84% of Zn(II)). Iron and zinc fractions were determined by quantitative analysis (electron microprobe analysis and CHN). The found and calculated values are in good agreement, as can be seen in **Figure 2**. The elemental analysis of C, H, N were performed on FlashEA^{TM} 1112, and the results agreed well with the calculated data. 6 compounds were obtained with x = 1 (**1.**2H$_2$O), x = 0.85 (**2.**2H$_2$O), x = 0.70 (**3.**2H$_2$O), x = 0.49 (**4.**2H$_2$O), x = 0.27 (**5.**2H$_2$O) and x = 0 (**6.**2H$_2$O). Elemental Anal (%) *Calc.* for compound **1.**2H$_2$O [Fe(pz)(Pt(CN)$_4$)].2H$_2$O C 20.38, H 1.71, N 17.83; *found* C 20.76, H 1.21, N 17.85. *Calc.* for compound **2.**2H$_2$O [Fe$_{0.85}$Zn$_{0.15}$(pz)(Pt(CN)$_4$)].2H$_2$O C 20.33, H 1.70, N 17.79; *found* C 19.84, H 1.26,

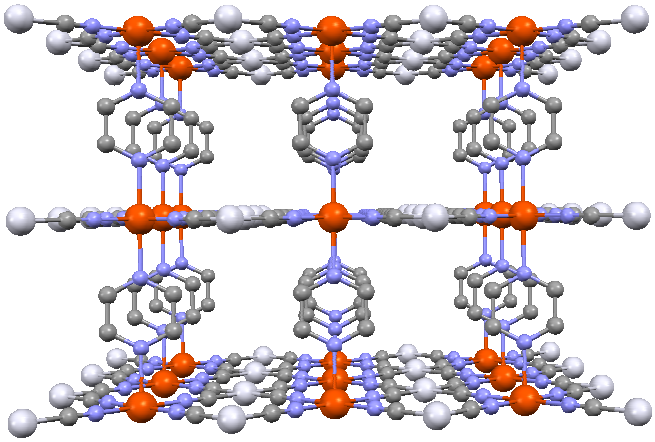

Figure 1: Perspective view of the structure of [Fe(pz)(Pt(CN)$_4$)]

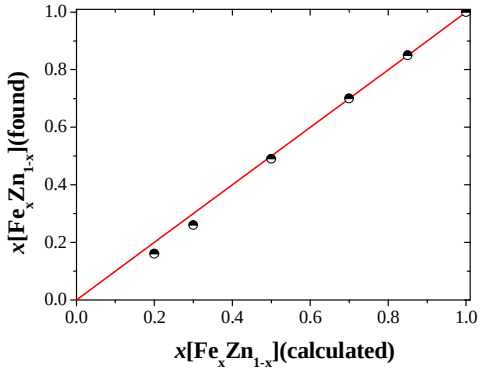

Figure 2: Iron fraction *x* obtained from elemental analysis *vs* iron fraction calculated from the iron/zinc ratio used for the synthesis. The full line corresponds to the ideal situation where *x*(found) = *x*(calculated).

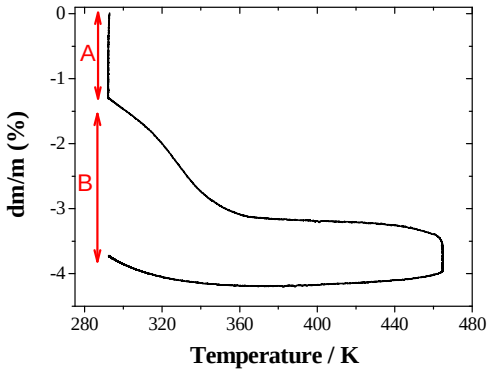

Figure 3: TGA measurement on complex $[Fe(pz)(Pt(CN)_4)].2H_2O$.

N 17.23; *Calc*. for compound **3.**$2H_2O$ $[Fe_{0.70}Zn_{0.30}(pz)(Pt(CN)_4)].2H_2O$ C 20.28, H 1.70, N 17.74; *found* C 20.32, H 1.16, N 17.55; *Calc*. for compound **4.**$2H_2O$ $[Fe_{0.49}Zn_{0.51}(pz)(Pt(CN)_4)].2H_2O$ C 20.20, H 1.69, N 17.68; *found* C 19.98, H 1.03, N 17.47. *Calc*. for compound **5.**$2H_2O$ $[Fe_{0.27}Zn_{0.73}(pz)(Pt(CN)_4)].2H_2O$ C 20.14, H 1.69, N 17.62; *found* C 19.68, H 1.37, N 17.05. *Calc.* for compound **6.**$2H_2O$ $[Zn(pz)(Pt(CN)_4)].2H_2O$ C 20.04, H 1.68, N 17.54; found C 19.19, H 1.61, N 16.53.

Before measurements, the samples were heated to 150 °C for 2 hours under nitrogen flux. Thermogravimetry analysis proved that this procedure was necessary to remove two water molecules. Differential thermal analysis has been performed on the neat compound $[Fe(pz)(Pt(CN)_4)].2H_2O$ using a mixt TG-DGA setup in the range of temperature 20-200 °C. **Figure 3** reports this experiment. A two-step thermal decomposition process was observed. The mass loss process starts at around 295 K and finishes at around 380 K. Total mass loss at 380 K corresponds to 2 water molecules. Based on this, it is reasonable to attribute the mass loss observed at room temperature to the water molecule adsorbed at the surface while the behavior recorded during the heating process corresponds to the water molecule into the crystal lattice.

2.2. X-Ray powder diffraction.

The X-ray powder diffraction of **1-6.**$2H_2O$ have been recorded on a Philips PW1820 diffractometer provided by PANalytical X'Pert, using a Bragg-Bentano geometry (λ = 1.5406 Å) from 5 to 50° at 0.02°/s.

2.3. Magnetic and Photomagnetic Studies.

Magnetic susceptibility data were collected using a Quantum Design MPMS 5 SQUID magnetometer under an applied field of 1 T.

All measurements were performed on homogenous polycrystalline samples and in the temperature range 10 to 290 K. Diamagnetic corrections for the sample holder and the material (using Pascal constants) were applied.

Photomagnetic measurements were performed using a Kr+ laser coupled *via* an optical fibre to the cavity of a MPMS-5S Quantum Design SQUID magnetometer operating at 2 T. It was noted that there was no change in the data due to heating of the sample. The suspended crystalline sample was prepared in a thin layer (~0.1 mg) to promote full penetration of the irradiated light. The sample mass was obtained by comparison with the thermal spin transition curve measured on a larger accurately weighed polycrystalline sample. The calculated mass is of course approximate, however the adequacy between the bulk and thin layer magnetic measurements is reasonable, taking into account the fact that the data correction of such low amount of sample is challenging. Our previously published standardized method for obtaining LIESST data was followed. [14,42,43] The sample was first slowly cooled to 10 K, ensuring that potential trapping of HS species at low temperatures did not occur.

Irradiation was carried out at a set wavelength and the power at the sample surface

was adjusted to 5 mW cm^{-2} to prevent surface heating. Once photo-saturation was reached, irradiation was ceased and the temperature increased at a rate of 0.3 K min^{-1} to ~100 K and the magnetization measured every 1 K to determine the *T*(LIESST) value [14,42,43] ; given by the extreme of the $\delta \chi_M T / \delta T$ *versus T* curve for the relaxation. The *T*(LIESST) value describes the limiting temperature above which the light-induced magnetic high-spin information is erased in a SQUID cavity.

In the absence of irradiation, the magnetism was also measured over the temperature range 10 – 350 K to follow the thermal spin transition and to obtain a low temperature baseline.

3. Results and discussion

Starting from the neat compound $[Fe(pz)(Pt(CN)_4)].2H_2O$, **1**.$2H_2O$, several solid solutions $[Fe_xZn_{1-x}(pyrazine)(Pt(CN)_4)].2H_2O$ were synthesized with x = 0.85 (**2**.$2H_2O$), x = 0.70 (**3**.$2H_2O$), x = 0.49 (**4**.$2H_2O$), x = 0.27 (**5**.$2H_2O$), as well as the neat material$[Zn(pz)(Pt(CN)_4)].2H_2O$, **6**.$2H_2O$. No single crystals of the solid solutions could have been obtained. The compositions were determined by elemental analysis, showing that the found and expected values (the ones calculated for the synthesis) are in good agreement (**Figure 2**). The powder X-Ray diffraction of the six compounds were recorded. We first recorded powder X-ray diffractograms for the two pure compounds. In **Figure 4a**, we can notice a difference between the diffractograms of pure iron and zinc materials. This difference indicates that the two complexes are not isostructural. A limit of miscibility of the zinc in the pure iron material is therefore expected. **Figure 4b** shows room temperature powder diffractograms in the range from 10° to 50° (in twice the Bragg angle) of the pure and diluted compounds. The presence of well-defined Bragg reflections in the pure Fe(II) and Zn(II) diluted samples proves that these samples consist of well-crystallized phases. Moreover, all the (*hkl*) reflections positions and relative intensities match for all compounds. For x smaller than 0.50, several additional peaks start to appears as a signature of the appearance of the pure Zn phase, despite no demixion was observed by microprobe spectroscopy. These findings show that all of these compounds are isostructural and that the character of solid solution $[Fe_xZn_{1-x}]$ can be assigned to the mixed crystals with some caution for **4** and **5** compounds.

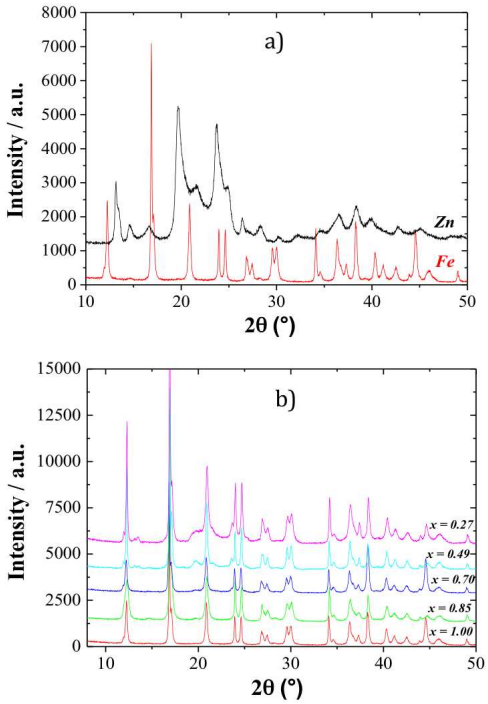

Figure 4: Room-temperature X-ray powder diffraction patterns of $Fe_xZn_{1-x}(pyrazine)[Pt(CN)_4]$ (a) (x = 1 and 0); (b) (x = 1, 0.85, 0.70, 0.49 and 0.27).

3.1. Magnetic characterization

The magnetic measurements were performed on the polycrystalline samples and the thermal evolution of the molar magnetic susceptibility, χ_M, was followed. The measured $\chi_M T$ product is, in fact, the sum of the contributions of iron(II) ions and zinc(II) ions (equation (1)). To have access to the behavior of the iron ions, the magnetic contribution of the zinc ion has been removed according to equation (2). Considering that the zinc(II) metal ions have a diamagnetic response ($(\chi_M T)_{Zn} = 0$) with regard to the filled $3d^{10}$ level, $(t_{2g})^6(e_g)^4$ and since the iron(II) ions in the LS state are diamagnetic ($\chi_M T)_{Fe}$ product is proportional to the HS fraction (γ_{HS}).

Thus, γ_{HS} may be directly deduced from the $(\chi_M T)_{Fe}$ product through equation (3) where $(\chi_M T)_{Fe}^{HT}$ refers to the neat iron compound ($x = 1$) at high temperatures, typically at ambient temperature. This value has been taken as 3.5 cm^3 K mol^{-1} for $[Fe(pz)(Pt(CN)_4)]$ as expected for a fully occupied quintet paramagnetic HS state (S = 2, $t_{2g}^4 e_g^2$). This value is, also, in good agreement with that expected from the Curie law ($\chi_M T = \frac{1}{8} . g^2 S(S+1)$) if a Lande factor of g = 2.2 is attributed to the iron(II) high spin ion. **Figure 5a** reports the thermal dependence of the $\chi_M T$ product for the desolvated mixed crystal system $[Fe_xZn_{1-x}(pz)(Pt(CN)_4)]$ (**1-5**).

$$\chi_M T = x(\chi_M T)_{Fe} + (1-x)(\chi_M T)_{Zn} \quad (1)$$

$$(\chi_M T)_{Fe} = \frac{\chi_M T - (1-x)(\chi_M T)_{Zn}}{x} \quad (2)$$

$$\gamma_{HS} = \frac{(\chi_M T)_{Fe}}{(\chi_M T)_{Fe}^{HT}} \quad (3)$$

It is well-known that the observation of a hysteresis loop is the consequence of the presence of a first-order phase transition. In that case, the equilibrium temperature ($T_{1/2}$) is replaced by the critical temperatures $T_{1/2}\downarrow$ and $T_{1/2}\uparrow$, defined as the temperature where γ_{HS} = 1/2 in the cooling and heating modes, respectively. The evolution of the spin transition temperatures, $T_{1/2}$, as a function of x in the cooling and heating modes in the $[Fe_xZn_{1-x}]$ mixed-crystal series are summarized in **Figure 5b** and listed in **Table I**. When x changes from 1.00 to 0.27, $T_{1/2}\downarrow$ varies from 282 to 237 K and $T_{1/2}\uparrow$ from 308 to 237 K. The hysteresis, which is 26 K for x = 1.00, vanishes for $x \leq 0.27$. If we assume, to a first approximation, that the spin equilibrium temperature can be expressed as $T_{eq} = (T_{1/2}\downarrow + T_{1/2}\uparrow)/2$, it appears that the value of T_{eq} decreases also with x (**Table I**). The information given by **Figure 5a** and **Figure 5b** agrees with the previous observations in metal dilution studies, [24-41] i.e. when the metal dilution increases, we can notice that, (i) the transition temperature $T_{1/2}$ shifts to lower temperatures which can be understood through change of internal pressure; (ii) spin crossovers become globally more gradual and (iii) the width of the hysteresis decreases and finally disappears reflecting a progressive loss of cooperativity. All that can be explained as a direct consequence of the negative pressure generated in the Zn host. In fact, it is now well-known that dilution with Zn stabilizes the HS state by inducing the so-called negative pressure. [24,41] Regarding the effects of metal dilution on the SCO behavior, let us point out the influence of the relative size of the inert metal ion. Indeed, our previous studies show that the larger the ion, the better stabilized the HS state, and consequently, the thermal transition is more rapidly shifted toward lower temperatures [35-37].

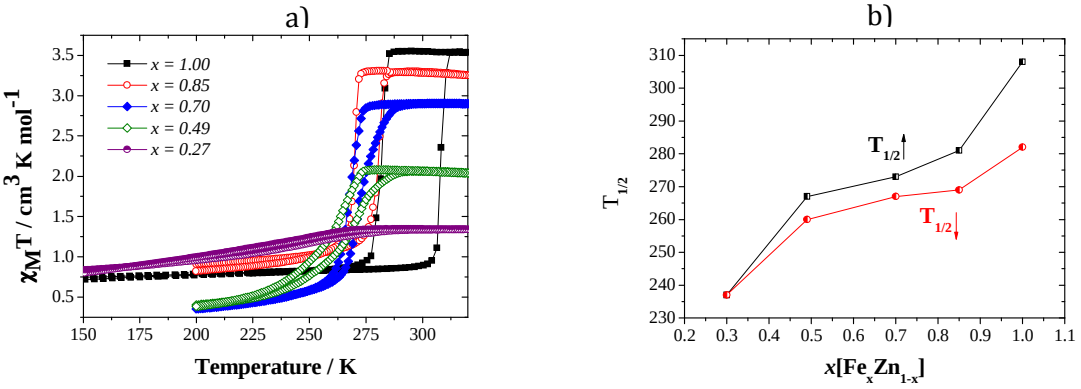

Figure 5: (a) Evolution of the $\chi_M T$ signal as function of x *vs.* T in the cooling and heating mode curves for $[Fe_xZn_{1-x}(pz)(Pt(CN)_4)]$ (b) Evolution of the spin transition temperatures as a function of x in the cooling (↓) and heating (↑) modes in $[Fe_xZn_{1-x}(pz)(Pt(CN)_4)]$.

3.2. Photomagnetic properties

The main novelty of the present work is the investigation of photomagnetic properties through LIESST investigation. The low → high spin photoconversion has been investigated in bulk conditions using a SQUID magnetometer coupled to a CW optical source. Irradiation of the different compounds has been realized at the following wavelengths: 510, 650, and 830 nm. For all the compounds, the most efficient wavelength to induce LIESST effect was found to be 510 nm, leading to an increase of the magnetic signal at 10 K. As expected regarding its weak lifetime, no photomagnetic effect was observed on compound **1**. **Figure 6** reports the photomagnetic experiments performed on **2-5**. For all 4 complexes, an increase in the magnetic signal under light irradiation was observed at 10 K. It should, however, be noticed that the amount of iron in the photo-excited high-spin state is not the same for all compounds and for none of the complexes it is quantitative. The percentage of photoconversion at 10 K was estimated by dividing the variation of $\chi_M T$ under irradiation by the variation of $\chi_M T$ due to the thermal SCO. Depending on the compound and the metal dilution, this percentage varies from 8 to 31. After light excitation at 10 K, the system was heated in the dark with a temperature increase rate of 0.3 $Kmin^{-1}$ to record the T(LIESST) curve. The $\chi_M T$ product first increases upon warming from 10-20 K due to zero-field splitting of the high spin iron(II) ion. [57] Then after a plateau, $\chi_M T$ value decreases sharply. To quantify the temperature at which the photoexcited state relaxes to the LS state, a limit temperature, T(LIESST), has been defined. T(LIESST) is defined as the minimum of the derivative $d(\chi_M T)/dT$ *vs.* T recorded during relaxation. Values of T(LIESST) are reported in **Table I**. For the samples of $[Fe_xZn_{1-x}(pyrazine)(Pt(CN)_4)]$, T(LIESST) has been recorded. The estimated T(LIESST) values are 45 K for x = 0.85; 26 K for x = 0.70; 31 K for x = 0.49 and 41 K for x = 0.27.

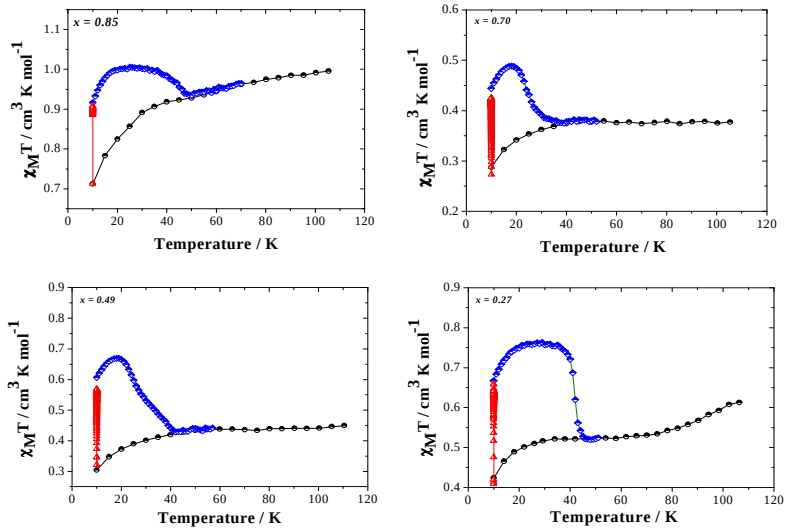

Figure 6: Temperature dependence of $\chi_M T$ for $[Fe_xZn_{1-x}(pyrazine)(Pt(CN)_4)]$ (○) = data recorded in warming modes without irradiation; (▲) = data recorded with irradiation at 532 nm at 10 K; (◊) = *T*(LIESST) measurement, data recorded in warming mode with the laser turned off after irradiation for one hour.

Table I. Magnetic and photomagnetic properties of the mixed $Fe_xZn_{1-x}(pyrazine)[Pt(CN)_4]$ system. $T_{1/2}$ is the temperature at which the sample contains 50% of LS and HS molecules. Teq = $(T_{1/2}\downarrow + T_{1/2}\uparrow)/2$. *T*(LIESST) is the temperature at which the light-induced HS information was erased during warming from 10 K at a rate of 0.3 K min^{-1}.

SCO Systems	$T_{½}\downarrow$ (K)	$T_{½}\uparrow$ (K)	T_{eq} *(K)*	*Hysteresis width (K)*	*T*(LIESST) (K)	*% Photoexcitation*
[Fe(pyrazine)(Pt(CN)$_4$)]	282	308	295	26	/	/
[$Fe_{0.85}Zn_{0.15}$(pyrazine)(Pt(CN)$_4$)]	269	281	275	12	45	8
[$Fe_{0.70}Zn_{0.27}$(pyrazine)(Pt(CN)$_4$)]	267	273	270	6	26	8
[$Fe_{0.49}Zn_{0.51}$(pyrazine)(Pt(CN)$_4$)]	260	267	263.5	7	31	17
[$Fe_{0.27}Zn_{0.73}$(pyrazine)(Pt(CN)$_4$)]	237	237	237	0	41	31

3.3. Discussion

Table I collects all the data obtained during this study. The main dilution effects observed for the mixed-crystal series $[Fe_xZn_{1-x}(pz)(Pt(CN)_4)]$, are in agreement with those observed earlier for the compound $[Fe_xM_{1-x}(pz)(Pt(CN)_4)]$, (M = Ni(II), Co(II)). [31] The dilution tends to smoothen the spin transition curves (**Figure 5a**), and the transition temperatures change also with the dilution (**Figure 5b**). The magnitude of this latter effect strongly depends on the nature of the diluting metal. [35-37] First of all, T_{eq} decreases by 58 K between the pure compound ($x = 1$) and the most diluted compound ($x = 0.27$). This is in agreement with those observed earlier on $[Fe_xCo_{1-x}(pz)(Pt(CN)_4)]$ series. [31] As far as photomagnetic properties are concerned, results show that T(LIESST) values and the level of percentage of photoconversion vary upon dilution. More precisely, the percentage of photoconversion, is in fact about 08% for $x = 0.85$ and $x = 0.70$; 17% for $x = 0.49$, and 31% for $x = 0.27$.

Regarding our objectives of this work, the increase of the photoconversion efficiency upon metal dilution appears to be successful. Indeed, in the pure iron compound, cooperativity is so important, that the rigidity of the structure could avoid an efficient light conversion by disfavoring the propagation of the inherent volume change upon LS $\rightarrow$ HS conversion. Since the metal dilution effect is first to weaken the cooperativity and secondly to favor the HS state through the internal pressure applied by the zinc ions, these two effects should favor the efficiency of the light excitation. These explanations seem to be reasonable for the actual observation in the present study. Let us note that incomplete photoconversions have already been observed in many SCO compounds [33,53,58,59] and usually, it was explained by a short penetration depth of the light during photoexcitation. With regards to this hypothesis, it is well known that metal dilution with zinc leads to a bleaching of the compound. Therefore, for highly metal-diluted samples, the penetration of light into the material should be facilitated and a higher degree of photoexcitation may be anticipated. This effect could take part to the observed increase of photoconversion.

In addition to this observation, metal dilution has a drastic effect on the occurrence of photoswitching on this $[Fe_xZn_{1-x}(pz)(Pt(CN)_4)]$ family. Indeed, introducing diluting ions allows to observe a photoconversion while, in the same experimental conditions, no effect was observed on the pure iron compound. Moreover, regarding the T(LIESST) values, they are difficult to compare regarding their variation upon metal dilution. This variation probably follows from two effects. The first one is the fact that the sample is desolvated *ex-situ* before inserting it in the SQUID magnetometer cavity. This transfer takes several minutes during which a small amount of water can be can caught leading to a mixing of phases. This could explain the presence of steps in the T(LIESST) curves. The second effect could be the fact that at the microscopic level, a local demixion of phases between a diluted phase and the pure $[Zn(pz)(Pt(CN)_4)]$ as suggested by the XRD powder diffractograms (Figure 4). Finally, with the hypothesis that the most pure sample is related to the smallest amount of zinc, we can discuss the T(LIESST) value of **2** with the ones reported in the literature on three dimensional networks derivate from the pure Hoffman phase that are close to 60 K. [54,56,60] The 45 K observed on **2** is obviously lower than this value.

4. Conclusions

The main objective of the present work was to study experimentally metal dilution effects on the thermal and light-induced spin transition of Iron(II) in the three-dimensional coordination polymer. To accomplish this goal, we decided to investigate Zn(II) metal dilution effects on $[Fe(pz)(Pt(CN)_4)]$ using magnetic and photomagnetic susceptibility measurements as well as powder X-ray diffraction (PXRD). The magnetic and photomagnetic behavior of these solids solutions revealed similar tendencies that can be observed in molecular spin-crossover complexes. We have reported the thermal and photo-induced spin-crossover properties of $[Fe_xZn_{1-x}(pyrazine)(Pt(CN)_4)]$ systems and compare these results to previous results. We have shown that dilution has a strong effect on magnetic and photomagnetic properties since metal dilution promoted light-induced SCO while it was not

observed on the pure compound in similar conditions.

Acknowledgements

We thank the Department of Cooperation and Cultural Action Embassy of France to Dakar-Sénégal, the University of Ziguinchor and its Department of Cooperation and Research, the Ministry of Higher Education and Research of Sénégal (Program FIRST) and CAMPUS France. This work was also supported by the University of Bordeaux, the CNRS, the Region Nouvelle Aquitaine and by the LabEx AMADEus (ANR-10-LABX-42) within IdEx Bordeaux (ANR-10-IDEX-03-02), i.e. the Investissements d'Avenir programme of the French government managed by the Agence Nationale de la Recherche. The ANR is also warmly acknowledge (ANR femtomat n° 13-BS04-002). The UMS PLACAMAT is acknowledged for the microprobe measurements.

References

[1] Gütlich P, Garcia Y, Goodwin HA. Spin crossover phenomena in Fe(II) complexes. Chem. Soc. Rev. (2000) 29, 419–427.

[2] Gütlich P, Goodwin HA. Spin crossover-An overall perspective. Top. Curr. Chem. (2004) 233, 1–47.

[3] Goodwin HA. Spin crossover in iron(II) tris(diimine) and bis(terimine) systems. Top. Curr. Chem. (2004) 233, 59–90.

[4] Long GJ, Grandjean F, Reger DL. Spin crossover in pyrazolylborate and pyrazolylmethane complexes. Top. Curr. Chem. (2004) 233 91–122.

[5] Toftlund H, McGarvey JJ. Iron(II) Spin crossover systems with multidentate ligands. Top. Curr. Chem. 233 (2004) 233, 151–166.

[6] Halcrow MA. Ed.; Spin-Crossover Materials: Properties and Applications; John Wiley & Sons: Chichester UK, 2013.

[7] Morscheidt W, Jeftic J, E Codjovi E, Linares J , Bousseksou A, Constant-Machado H, Varret F. Optical detection of the spin transition by reflectivity: application to $[Fe_xCo_{1-x}$ $(btr)_2(NCS)_2].H2O$. Meas. Sci. Technol. (1998) 9, 1311–1315.

[8] Gütlich P, Hauser A, Spiering H. Thermal and Optical Switching of Iron(II) Complexes. Angew. Chem. (1994) 33, 2024-2054.

[9] Gütlich P, Gaspar AB, Garcia Y. Spin state switching in iron coordination compounds. Beilstein J. Org. Chem. (2013) 9, 342–391.

[10] Guionneau P, Marchivie M, Bravic G, Létard JF, Chasseau D. Structural aspects of spin crossover: Example of the $[Fe^{II}L_n(NCS)_2]$ complexes. Top. Curr. Chem. (2004) 234, 97-126.

[11] Guionneau P. Crystallography and spin-crossover. A view of breathing materials. Dalton Trans. (2014) 43, 382–393.

[12] Kahn O, Kröber J, Jay Martinez C. Spin transition molecular materials for displays and data recording. Adv. Mater. (1992) 4, 718–728.

[13] Kahn O, Jay Martinez C. Spin-transition polymers: From molecular materials toward memory devices. Science. (1998) 279, 44–48.

[14] Létard JF, Guionneau P, Goux-Capes L. Towards spin crossover applications. Top. Curr. Chem. (2004) 235, 221–249.

[15] Molnar G, Salmon L, Nicolazzi W, Terki F, Bousseksou A. Emerging properties and applications of spin crossover nanomaterials. J. Mater. Chem. C. (2014) 2, 1360-1366.

[16] Aragonès AC, Aravena D, Cerdà JI, Acis-Castillo Z, Li H, Real JA, Sanz F, Hihath J, Ruiz E, Diez-Perez I. Large Conductance Switching in a Single-Molecule Device through Room Temperature Spin-Dependent Transport. Nano Lett. (2016) 16, 218-226.

[17] Bertoni R, Cammarata M, Lorenc M, Matar S, Létard JF, Lemke HT, Collet E. Ultrafast Light-Induced Spin-State Trapping Photophysics Investigated in $Fe(phen)_2(NCS)_2$ Spin-Crossover Crystal. Acc. Chem. Res. (2015) 48, 774-781.

[18] Descurtins S, Gütlich P, Köhler CP, Spiering H, Hauser A. Light-induced excited spin state trapping in a transition-metal complex: The hexa-1-propyltetrazole-iron(II) tetrafluoroborate spin-crossover system. Chem. Phys. Lett. (1984) 105, 1–4.

[19] McGarvey JJ, Lawthers I. Photochemically-induced perturbation of the $^1A \rightleftharpoons {}^5T$ equilibrium in Fe^{11} complexes by pulsed laser irradiation in the metal-to-ligand charge-transfer absorption band. J. Chem. Soc., Chem. Comm. (1982) 16, 906-907.

[20] Hauser A. Reversibility of light-induced excited spin state trapping in the Fe(ptz)6(BF4)2, and the $Zn_{1-x}Fe_x(ptz)_6(BF4)_2$ spin-crossover systems. Chem. Phys. Lett. (1986) 124, 543-548.

[21] Matsuda H, Tajima H. patent no JP2009212164 A. (2009).

[22] Sato O. Optically Switchable Molecular Solids: Photoinduced Spin-Crossover, Photochromism, and Photoinduced Magnetization. Acc. Chem. Res. (2003) 36, 692-700.

[23] Molecular Switches, 2nd ed. (Eds. B. Feringa, W. R. Browne), Wiley-VCH, Weinheim (Germany), (2011).

[24] Ganguli P, Gütlich P, Müller EW. Effect of metal dilution on the spin-crossover behavior in $[Fe_xM_{1-x}(phen)_2(NCS)_2]$ (M = Mn, Co, Ni, Zn). Inorg. Chem. (1982) 21, 3429–3433.

[25] Haddad MS, Federer WD, Lynch MW, Hendrickson DN. An explanation of unusual properties of spin-crossover ferric complexes. J. Am. Chem. Soc. (1980) 102, 1468–1470.

[26] Haddad MS, Federer WD, Lynch MW, Hendrickson DN. Spin-crossover ferric complexes: Unusual effects of grinding and doping solids. Inorg. Chem. (1981) 20, 131–113.

[27] Varma V, Fernàndes JR. An infrared spectroscopy study of the low-spin-high-spin transition in $[Fe_xM_{1-x}(phen)_2(NCS)_2]$. A composition-induced change in the order of the spin-state transition. Chem. Phys. Lett. (1990) 167, 367–370.

[28] Martin JP, Zarembowitch J, Dworkin A, Haasnoot JG, Varret F. Solid-state effects in spin transitions: Influence of iron(II) dilution on the magnetic and calorimetric properties of the series Fe_xNi_{1-x}(4,41-bis(1,2,4-triazole))$_2(NCS)_2$].cntdot.H_2O. Inorg. Chem. (1994) 33, 2617–2623.

[29] Martin JP, Zarembowitch J, Bousseksou A, Dworkin A, Haasnoot JG, Varret F. Solid state effects on spin transitions: Magnetic, calorimetric, and Mossbauer-effect properties of $[Fe_xCo_{1-x}(4,41\text{-bis}(1,2,4\text{-triazole}))_2(NCS)_2]$.cntdot.$H_2O$ mixed-crystal compounds. Inorg. Chem. (1994) 33, 6325–6333.

[30] Niel V, Martinez-Agudo JM, Carmen Munoz M, Gaspar AB, Real JA. Cooperative Spin Crossover Behavior in Cyanide-Bridged Fe(II)-M(II) Bimetallic 3D Hofmann-like Networks (M) Ni, Pd, and Pt). Inorg. Chem. (2001) 40, 3838-3839.

[31] Tayagaki T, Galet A, Molnar G, Carmen Munoz M, Zwick A, Tanaka K, Real JA, Bousseksou A. Metal Dilution Effects on the Spin-Crossover Properties of the Three-Dimensional Coordination Polymer $Fe(pyrazine)[Pt(CN)_4]$ J. Phys. Chem. B. (2005) 109, 14859-14867.

[32] Baldé C, Desplanches C, Wattiaux A, Guionneau P, Gütlich P, Létard JF. Effect of metal dilution on the light-induced spin transition in $[Fe_xZn_{1-x}(phen)_2(NCS)_2]$ (phen = 1,10-phenanthhroline). Dalton Trans. (2008) 2702–2707.

[33] Baldé C, Desplanches C, Grunert M, Wei Y, Gütlich P, Létard JF. Influence of metal dilution on the light-induced spin transition in two 1D chain compounds: $[Fe_xZn_{1-x}(btzp)_3](BF4)_2$ and $[Fe_xZn_{1-x}(endi)_3](BF4)_2$ {btzp = 1,2-bis(tetrazol-1-yl)propane and endi = 1,2-Bis(tetrazol-1-yl)ethane}. Eur. J. Inorg. Chem. (2008) 5382–5389.

[34] Baldé C, Desplanches C, Gütlich P, Freysz E, Létard JF. Effect of the metal dilution on the thermal and light-induced spin transition in $[Fe_xMn_{1-x}(bpp)_2](NCSe)_2$: When T(LIESST) reaches $T_{1/2}$. Inorg. Chim. Acta (2008) 361, 3529–3533.

[35] Baldé C, Desplanches C, Le Gac F, Guionneau P, and Létard JF. The role of iron(II) dilution in the magnetic and photomagnetic properties of the series $[Fe_xZn_{1-x}(bpp)_2](NCSe)_2$. Dalton Trans. (2014) 43 , 7820-7829.

[36] Baldé C, Desplanches C, Létard JF, Chastanet G. Effects of metal dilution on the spin-crossover behavior and light induced bistability of iron(II) in $[Fe_xNi_{1-x}(bpp)_2](NCSe)_2$. Polyhedron (2017) 123, 138–144.

[37] Sylla MS, Baldé C, Daro N, Desplanches C, Marchivie M, Chastanet G. On the Role of the Internal Pressure on the Photo-Induced Spin-Crossover behavior of $[Fe_xM_{1-x}(phen)_2(NCS)_2]$ solid solutions (M=Ni(II), Zn(II) and Cd(II)). Eur. J. Inorg. Chem. 10.1002/ejic.201700350. (2017).

[38] Paradis N, Chastanet G, Létard JF. When stable and metastable HS states meet in spin-crossover compounds. Eur. J. Inorg. Chem. (2012) 3618–3624.

[39] Paradis N, Chastanet G, Varret F, Létard JF. Metal dilution of cooperative spin-crossover compounds: When stable and metastable high-spin states meet. Eur. J. Inorg. Chem. (2013) 968–974.

[40] Paradis N, Le Gac F, Guionneau P, Largeteau A, Yufit DS, Rosa P, Létard JF, Chastanet G. Effects of Internal and External Pressure on the $[Fe(PM\text{-}PEA)_2(NCS)_2]$ Spin-Crossover Compound (with PM-PEA = N-(21-pyridylmethylene)-4-(phenylethynyl)aniline). Magnetochemistry (2016) 2, 15.

[41] Chakraborty P, Enachescu C, Walder C, Bronisz R and Hauser A. Thermal and Light-Induced Spin Switching Dynamics in the 2D Coordination Network of $\{[Zn_{1-x}Fe_x(bbtr)_3](ClO4)_2\}_\infty$: The Role of Cooperative Effects. Inorg. Chem. (2012) 51, 9714−9722.

[42] Létard JF, Capes L, Chastanet G, Moliner N, Létard S, Real JA, Kahn O. Critical temperature of the LIESST effect in iron(II) spin-crossover compounds. Chem. Phys. Lett. (1999) 313, 115–120.

[43] Létard JF, Chastanet G, Guionneau P, Desplanches C. Optimising the stability of trapped metastable spin states. In Spin-Crossover Materials - Properties and Applications; Halcrow, M.A., Ed.; John Wiley & Sons: Chichester, UK, (2012); pp. 475–506.

[44] Hauser A. Light-induced spin-crossover and the high spin-low spin relaxation. Top. Curr. Chem. (2004) 234, 155–198.

[45] Hauser A, Enachescu C, Daku ML, Vargas A, Amstutz N. Low-temperature lifetimes of metastable high-spin states in spin-crossover and in low-spin iron(II) compounds: The rule and exceptions to the rule. Coord. Chem. Rev. (2006) 250, 1642–1652.

[46] Létard JF, Chastanet G, Nguyen O, Marcén S, Marchivie M, Guionneau P, Chasseau D, Gütlich P. Spin Crossover Properties of the $[Fe(PM\text{-}BiA)_2(NCS)_2]$ Complex – Phases I and II. Monatsh. Chem. (2003) 134, 165-182.

[47] Hayami S, Gu ZZ, Einaga Y, Kobayashi Y, Ishikawa Y, Yamada Y, Fujishima A, Sato O. A Novel LIESST Iron(II) Complex Exhibiting a High Relaxation Temperature. Inorg. Chem. (2001) 40, 3240-3242.

[48] Costa JS, Guionneau P, Létard JF. Photomagnetic properties of the $[Fe(L_{222}(N_3O_2))(CN)_2]$centerdot$H_2O$ complex: a fascinating example of multi-metastability J. Phys.: Conference Series. (2005) 21, 67-72.

[49] Shimamoto N, Ohkoshi S, Sato O, Hashimoto K. Control of charge-transfer-induced spin transition temperature on cobalt-iron Prussian blue analogues. Inorg. Chem. (2002) 41, 678-684.

[50] Le bris R, Mathonière C, Létard JF. Cooperative relaxation of the metastable states in the photomagnetic octacyanotungstate $Cs^I[\{Co^{II}(3\text{-}CN\text{-}py)_2\}\{WV(CN)_8\}]\cdot H_2O$. Chem. Phys. Lett. (2006) 426, 380-386.

[51] Li D, Clérac R, Roubeau O, Harte E, Mathonière C, Le Bris R, Holmes SM. Magnetic and Optical Bistability Driven by Thermally and Photoinduced Intramolecular Electron Transfer in a Molecular Cobalt−Iron Prussian Blue Analogue. J. Am. Chem. Soc. (2008) 130, 252-258.

[52] Paez-Espejo M, Sy M, Boukheddaden K. Elastic Frustration Causing Two-step and Multi-Step Transitions in Spin Crossover Solids: Emergence of complex Antiferroelastic Strucures, J. Am. Chem. Soc. (2016) 136, 3202-3210.

[53] Baldé C, Bauer W, Kaps E, Neville S, Desplanches C, Chastanet G, Weber B, and Létard JF. Light-Induced Excited Spin-State Properties in 1D Iron(II) Chain Compounds. Eur. J. Inorg. Chem. (2013) 2744–2750.

[54] Sciortino NF, Scherl-Gruenwald KR, Chastanet G, Halder GJ, Chapman KW, Létard J-F, Kepert CJ, Hysteretic Three-Step Spin Crossover in a Thermo- and Photochromic 3D Pillared Hofmann-type Metal–Organic Framework, Angew. Chem. Int. Ed., Engl. (2012) 51, 10154-10158.

[55] Delgado T, Tissot A, Besnard C, Guénée L, Pattison P, Hauser A. Structural Investigation of the High Spin → Low Spin Relaxation Dynamics of the Porous Coordination Network $[Fe(pz)Pt(CN)_4]\cdot 2.6H_2O$. Chem. Eur. J. (2015) 21, 3664-3670.

[56] Ragon F, Yaksi K, Sciortino NF, Chastanet G, Létard J.-F, D'Alessandro DM, Kepert CJ, Neville SM, Thermal Spin Crossover Behaviour of Two-Dimensional Hofmann-Type Coordination Polymers Incorporating Photoactive Ligands. Aust. J. Chem. (2014) 67, 1563-1573.

[57] Kahn O. Molecular Magnetism, VCH, Weinheim, Germany, 1993.

[58] Absmeier A, Bartel M, Carbonera C, Jameson G, Weinberger P, Caneschi A, Mereiter K, Létard JF, Linert W. Both Spacer Length and Parity Influence the Thermal and Light-Induced Properties of Iron(II) α,ω-Bis(tetrazole-1-yl)alkane. Coordination Polymers. Chem. Eur. J. (2006) 12, 2235–2243.

[59] Absmeier A, Bartel M, Carbonera C, Jameson G, Werner F, Reissner M, Caneschi A, Létard JF, Linert W. Mutual Influence of Spacer Length and Noncoordinating Anions on Thermal and Light-Induced Spin-Crossover Properties of Iron(II)–α,ω-Bis(tetrazol-1-yl)alkane. Coordination Polymers. Eur. J. Inorg. Chem. (2007) 19, 3047–3054.

[60] Sciortino NF, Neville SM, Létard JF, Moubaraki B, Murray KS, Kepert CJ. Thermal- and Light-Induced Spin-Crossover Bistability in a Disrupted Hofmann-Type 3D Framework. Inorg. Chem. (2014) 53, 7886-7893.